THE JOURNAL OF



pubs.acs.org/JPCA Article

Proton Transfer in a Bare Superacid—Amine Complex: A Microwave and Computational Study of Trimethylammonium Triflate

Published as part of The Journal of Physical Chemistry virtual special issue "125 Years of The Journal of Physical Chemistry".

Nathan Love, Anna K. Huff, and Kenneth R. Leopold*



Cite This: J. Phys. Chem. A 2021, 125, 5061-5068



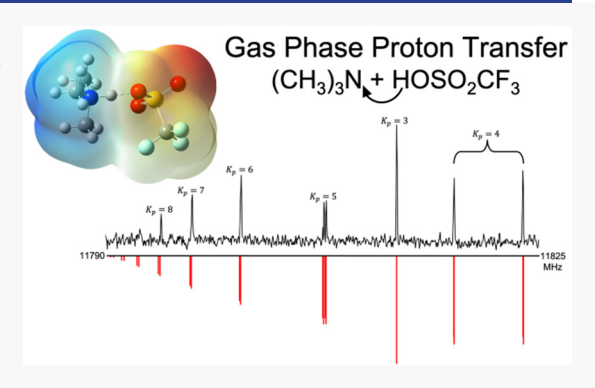
ACCESS

III Metrics & More

Article Recommendations

Supporting Information

ABSTRACT: The complex formed from trimethylamine ((CH₃)₃N) and trifluoromethanesulfonic acid (triflic acid, CF₃SO₃H) has been observed by Fourier transform microwave spectroscopy in a supersonic jet. Spectroscopic data, most notably 14N nuclear quadrupole coupling constants, are combined with computational results at several levels of theory to unambiguously demonstrate complete or near-complete proton transfer from the triflic acid to the trimethylamine upon complexation. Thus, the system is best regarded as a trimethylammonium triflate ion pair in the gas phase. The formation of an isolated ion pair in a 1:1 complex of a Brønsted acid and base is unusual and likely arises due to the strong acidity of triflic acid. Simple energetic arguments based on proton affinities and the Coulomb interaction energy can be used to rationalize this result.



INTRODUCTION

Proton transfer is a simple and ubiquitous chemical reaction whose influence spans industrial to atmospheric to biological chemistry. Most proton transfer events in these arenas occur in the solution phase, and an interesting question concerns the role of solvation in facilitating the process. Cluster science has long sought to examine this question in the context of small molecular clusters, whose "solvation numbers" range from zero to "several". The majority of these studies indicate that for Brønsted acid-base pairs that readily undergo proton transfer under bulk conditions the corresponding bare molecular complexes fail to do so and are best described as hydrogenbonded systems.

Numerous techniques have been brought to bear on the question of proton transfer in isolated acid-base complexes, with amine-hydrogen halide systems playing a prototypical role. These include, but are not limited to, early cluster beam experiments, 2,3 negative ion photoelectron spectroscopy, 4,5 and numerous ab initio and density functional theory studies. 6-16 Most closely related to this work is a classic series of microwave studies by Legon and co-workers which has brought into particularly sharp focus the differences between proton transfer in clusters and condensed phase.¹⁷ Using amine-hydrogen halide complexes as prototypes, these workers used indicators such as ¹⁴N nuclear quadrupole coupling and centrifugal distortion constants to assess whether the R₃NH⁺X⁻ ion pair exists in an isolated complex. The quadrupole coupling tensor depends on the electric field

gradient at the nucleus arising from all extra-nuclear charges and is therefore acutely sensitive to the electronic environment at the ¹⁴N nucleus. Because the electronic environment at the nitrogen nucleus becomes more symmetrical when R₃N is transformed into R₃NH⁺, the quadrupole coupling constants tend toward zero, rendering them useful probes of proton transfer. While the bulk phase reaction of $R_3N(g)$ and HX readily form crystalline R₃NH⁺X⁻(s), complexes involving NH₃ were found to be hydrogen-bonded systems, e.g., H₃N··· HX. For trimethylamine, only the strongest acids, HBr and HI, formed complexes which were best described as ion pairs. The effect of adding one HF molecule to the gas phase H₃N···HF complex to form H₃N···(HF)₂ has also been explored by rotational spectroscopy, with the result that the added HF drives the system in the direction of proton transfer but does not induce gas phase ion pair formation.¹⁸ Collectively, these results speak to the importance of both acid strength and local environment in determining whether or not proton transfer will take place.

Microwave studies involving complexes of HNO3 with NH_3^{19} and trimethylamine²⁰ (TMA = $(CH_3)_3N$) have also

Received: April 13, 2021 Revised: May 17, 2021 Published: June 7, 2021





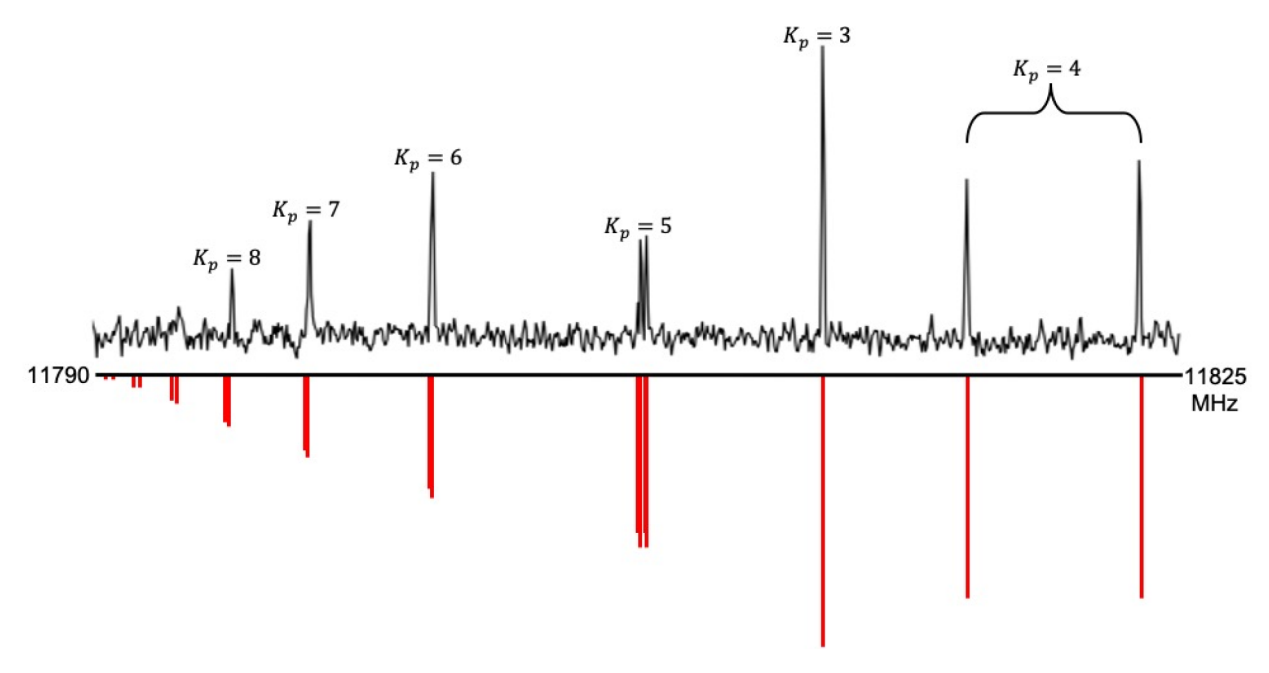


Figure 1. A portion of the chirped-pulse microwave spectrum of trimethylammonium triflate resulting from the average of 40,000 free induction decay signals, each collected for 20 μ s. The final fitted hyperfine frequencies are shown below as a stick spectrum. The transitions are all members of a pair of $J=12\leftarrow11$ a-type transitions with the same K_p value (e.g., $12_{5,7}\leftarrow11_{5,6}$ and $12_{5,8}\leftarrow11_{5,7}$) whose splitting decreases as K_p increases. For $K_p=6-8$, the two transitions are near perfectly overlapped. For K_p values in the 3–5 range, the individual transitions are resolvable with the chirped-pulse method. The second member of the $K_p=3$ pair appears at a frequency higher than 11825 MHz.

been reported. For these systems, the degree of proton transfer was again gauged by differences in the H14NO3 nuclear quadrupole tensor upon complexation with the result that in the TMA complex the proton transfer is ~62% complete. The ¹⁴N coupling tensor for the TMA, however, suggests a degree of proton transfer of only 31%, underscoring that the "degree" of proton transfer is defined only by the method used to measure it. Nevertheless, various measures of proton transfer, including bond distance and calculated infrared frequencies, paint a similar picture. Hydrated complexes of other strong acids, e.g., $HNO_3 - (H_2O)_{n=1-3}^{21-23} + HCl - (H_2O)_{n=1,2}^{24,25}$ $(HCl)_2 - H_2O_2^{-26} + HBr - (H_2O)_{n=1,2}^{27,28}$ and $HI - H_2O_2^{-29}$ have also been studied by microwave methods with an eye toward exploring the effect of hydration and microsolvation on proton transfer. A more extensive set of references, including those to both calculations and other types of experiments, may be found in ref 1.

In this paper, we further explore the influence of acidity on proton transfer in the gas phase. To do so, we report a microwave and computational study of the complex formed from TMA and the "superacid" triflic acid (trifluoromethane-sulfonic acid, CF_3SO_3H). Superacids are compounds with a higher (more negative) Hammett acidity function $(H_0)^{30}$ than pure sulfuric acid $(H_0 = -12)$ or for which the chemical potential of the acidic proton is greater than that of pure sulfuric acid. ^{31–33} Triflic acid is one of the most readily available superacids, with reports of its H_0 value in the -13.7 to -14.1 range, ^{32,34} thus making it about 100 times more acidic than sulfuric acid. ³⁴ Though highly corrosive, it is a relatively safe superacid to work with and finds numerous applications in synthetic chemistry. ^{32,35}

■ EXPERIMENTAL METHODS AND RESULTS

Spectra were taken on a pulsed-nozzle Fourier transform microwave spectrometer^{36,37} with broadband (chirped-

pulse)³⁸ and high-resolution (cavity)³⁹ capabilities. Transitions in the broadband and high-resolution systems were measured to accuracies of 12 and 3 kHz, respectively. To prepare the complex, a 0.5% mixture of TMA in argon was pulsed into the system at a stagnation pressure of 1.0 atm through a 0.8 mm diameter stainless steel cone nozzle. Triflic acid was introduced into the system by entraining the acid vapor in a 0.6 atm argon flow over an ~1.5 mL sample contained in a reservoir a short distance away from the nozzle. The resulting triflic acid/Ar mixture was then injected into the expanding gas plume through a 0.016 in. ID stainless steel needle that was inserted into the cone nozzle, as described previously. 40,41 The formation of the trimethylammonium triflate ion pair occurred during the on-the-fly mixing of the triflic acid/Ar and TMA/Ar gas mixtures, as evidenced by the resulting spectra and by the formation of small, yellowish crystals around the end of the stainless steel needle.

A broadband spectrum was initially collected in 3 GHz segments between 6 and 18 GHz. A portion of the spectrum is shown in Figure 1. Because of the small ¹⁴N nuclear hyperfine constants and the relatively high J levels accessed, the nuclear hyperfine structure was not resolvable at this stage, but a preliminary analysis using approximate line centers was, nevertheless, possible. Initial assignments were readily obtained in under 3 min using the DAPPERS package⁴² which was able to assign and fit 26 R-branch a-type transitions with $K_n \leq 2$ between J = 6 and 16 by using a semirigid rotor Hamiltonian. The resulting constants were highly predictive of the remaining 419 a- and b-type rotation-hyperfine transitions that were subsequently observed and measured with the cavity system. The a-type transitions were typically ~20-30 times stronger than the b-type lines. A few searches were conducted for predicted *c*-type transitions, but none were observed. However, this was expected given the small value of μ_c (0.2 D, see next section) and the signal-to-noise ratios obtained for the a- and b-type lines. A representative cavity spectrum with resolved ¹⁴N hyperfine structure is shown in Figure 2. The observed

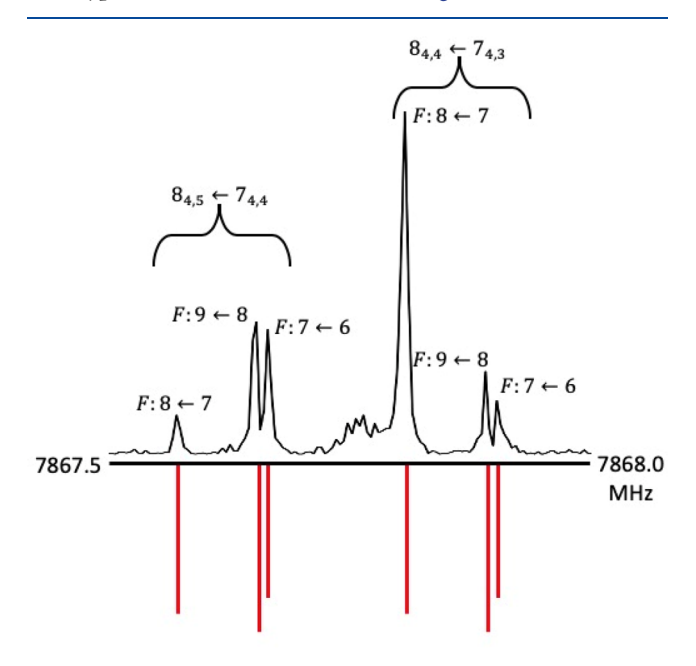


Figure 2. Cavity spectrum of resolved hyperfine components of a pair of high- K_n transitions resulting from the average of 400 free induction decay signals each collected for 205.5 µs. The stick spectrum shown below represents the frequencies obtained from the final fit.

frequencies were fit to a Watson A-reduced Hamiltonian, and the resulting rotational, distortion, and ¹⁴N hyperfine constants are given in Table 1. Their predicted values at the MP2/6-311++G(df,pd) level of theory are also included in the table. Further details of the calculations and a more complete set of computational results are presented below.

Table 1. Experimental and Computational Results for Trimethylammonium Triflate

	experimental	MP2/6-311++G(df,pd)	% difference
A (MHz)	1358.28926(38)	1358	0.02
B (MHz)	513.700508(88)	517	-0.64
C (MHz)	468.210731(85)	471	-0.60
Δ_I (kHz)	0.05857(49)		
Δ_{JK} (kHz)	-0.0885(27)		
Δ_K (kHz)	0.379(16)		
δ_I (kHz)	0.01087(36)		
δ_K (kHz)	0.100(30)		
χ_{aa} (MHz)	-1.5170(15)	-1.56	-2.8
χ_{bb} (MHz)	0.8047(19)	0.83	-3.1
χ_{cc} (MHz)	0.7124(19)	0.74	-3.9
N^a	419 (246)		
no. of a type	$365(109)^{b}$		
no. of b type	54(17) ^b		
RMS (kHz)	2.6		

^aNumber of transitions in the least-squares fit. Number in parentheses denotes the number of distinct frequencies. ^bNumber of transitions of the indicated type, including hyperfine components. The number in parentheses is the number of distinct rotational transitions.

■ COMPUTATIONAL METHODS AND RESULTS

B3LYP, M06-2X, and MP2 geometry optimization and frequency calculations were performed with varying basis sets for the trimethylammonium triflate complex, triflic acid, and trimethylamine. All calculations were performed by using Gaussian16.43 A comparison of the results of these calculations, both with each other and with the available experimental data, is shown in Table 2. The method/basis set in best agreement with A and B rotational constants was MP2/ 6-311++G(df,pd), which produced values accurate to 0 and 3 MHz, respectively. For the C rotational constant, the M06-2X/ 6-311++G(d,p) level/basis set performed slightly better than MP2/6-311++G(df,pd), with the two methods reproducing the experimental value to within 2 and 3 MHz, respectively. Note that, overall, both methods outperformed the B3LYP calculations. While both the MP2 and M06-2X results are in reasonable agreement with experiment, the MP2/6-311+ +G(df,pd) calculations are, for the most part, in somewhat better agreement with observed values. Therefore, this was the method chosen for further computational analysis in this work. The a, b, and c dipole moments calculated at the MP2/6-311+ +G(df,pd) are 10.6, 3.9, and 0.2 D, respectively, and the nuclear quadrupole coupling constants, χ_{aa} , χ_{bb} , and χ_{cc} , are within 4% of the observed values. The optimized structure is shown in Figure 3, and the Cartesian coordinates for this predicted structure are included in the Supporting Information. The binding energy for the complex at the MP2/6-311+ +G(df,pd) level was determined to be -31.4 kcal/mol (-29.1)kcal/mol after zero-point energy corrections). A one-dimensional potential was also calculated by fixing the N-H distance at a series of values and reoptimizing the energy with respect to all remaining structural parameters. The resulting potential function is shown in Figure 4. Figure 5 shows an electrostatic potential map on the electron density surface, where red regions represent more negative charge and blue represent regions represent more positive charge.

Finally, as noted above, the ¹⁴N nuclear quadrupole coupling tensor depends on the electric field gradient at the nitrogen nucleus due to extranuclear charges, and thus the measured quadrupole coupling constants were expected to be sensitive to the location of the proton in the complex. Thus, χ_{aa} , χ_{bb} , and χ_{cc} were calculated at the MP2/6-311++G(df,pd) level at each of the N-H distances represented in Figure 4. Figure 6 shows the resulting values. The experimental hyperfine constants are indicated by squares that have been placed at the nitrogenhydrogen distance obtained from the fully optimized structure (1.093 Å) and are seen to be in excellent agreement with those calculated at that distance.

DISCUSSION

The body of both experimental and theoretical evidence obtained in this work indicates that the complex formed from triflic acid and trimethylamine in a cold supersonic jet is best described as a trimethylammonium triflate ion pair, (CH₃)₃NH⁺···O₃SCF₃⁻. As described below, the strongest experimental evidence comes from the observed nuclear quadrupole coupling constants, while the computational results provide both supporting and independent information.

If the complex were weakly bound, the standard approach to interpreting the observed nuclear quadrupole coupling constants would involve examination of the projections of the coupling constants of free TMA (assumed to be

Table 2. Computational Results for Trimethylammonium Triflate

	B3LYP	M06-2X	MP2	
	6-311++G(d,p)	6-311++G(d,p)	6-311++G(d,p)	
	6-311++G(df,pd)	6-311++G(df,pd)	6-311++G(df,pd)	observed ^a
A (MHz)	1356	1352	1346	1358
	1357	1352	1358	
B (MHz)	479	518	509	514
	481	521	517	
C (MHz)	440	470	464	468
	442	473	471	
$R(N-H) (Å)^b$	1.08	1.08	1.08	
	1.08	1.08	1.09	
$R(O-H) (Å)^c$	1.54	1.51	1.49	
	1.53	1.50	1.46	
\angle (N-H-O) (deg)	178.9	178.6	178.5	
	179.3	178.8	176.9	
$ ho_{PT}$ (Å)	0.51	0.48	0.47	
	0.50	0.48	0.43	
$\Delta E ext{ (kcal/mol)}$	-26.7	-32.1	-31.7	
	-26.1	-31.4	-31.4	
$\Delta E_{ m ZP}$ (kcal/mol)	-23.8	-29.7	-29.0	
	-23.2	-29.0	-29.1	
χ_{aa} (MHz)	-1.49	-1.33	-1.46	-1.5170(15)
	-1.54	-1.36	-1.56	
$\chi_{bb}~({ m MHz})$	0.87	0.74	0.791	0.8047(19)
	0.89	0.74	0.83	
χ _{cc} (MHz)	0.62	0.59	0.67	0.7124(19)
	0.65	0.63	0.74	
μ_a (D)	10.6	10.1	10.2	
	10.6	10.0	9.9	
μ_b (D)	3.9	3.9	3.8	
	3.9	4.0	3.5	
μ_c (D)	0.2	0.2	0.2	
	0.2	0.2	0.2	
$\mu_T (D)^d$	11.3	10.8	10.9	
	11.3	10.8	10.5	

^aValues expressing the full measurement accuracy are given in Table 1. ^bThe calculated distance in TMAH⁺ at the MP2/6-311++G(df,pd) level is 1.024 Å. ^cThe calculated distance in free triflic acid at the MP2/6-311++G(df,pd) level is 0.967 Å. ^dTotal dipole moment = $\sqrt{\mu_a^2 + \mu_b^2 + \mu_c^2}$.

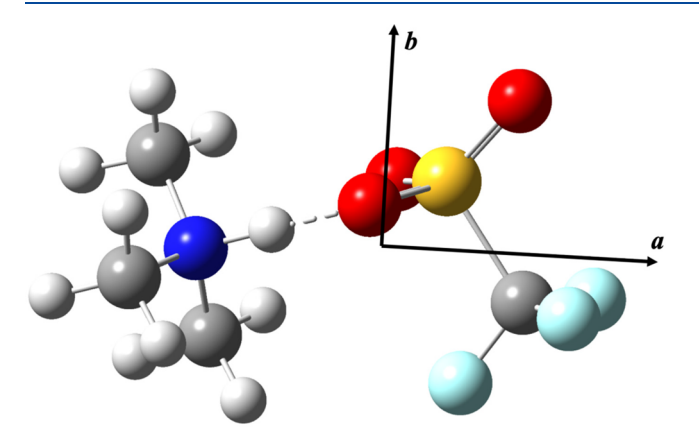


Figure 3. Optimized structure of trimethylammonium triflate obtained with MP2/6-311++G(df,pd) calculations. The orientation of the a- and b-inertial axes is shown. The a- and b-axes are in the plane of the page, and the origin is drawn at the center of mass of the complex.

unperturbed upon complexation) onto the inertial axis system of the complex. However, projection of the known quadrupole

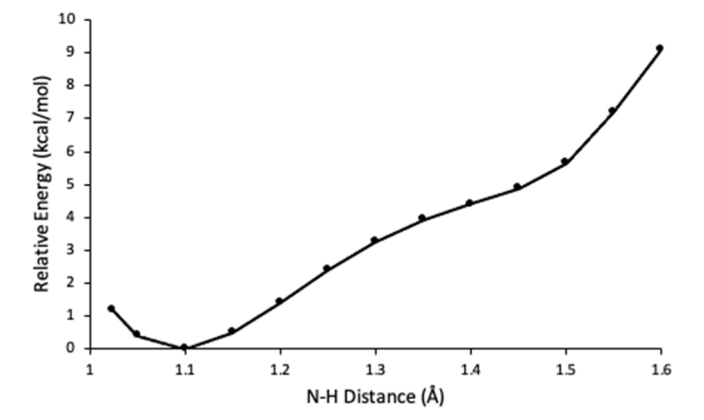


Figure 4. Energy of the $CF_3SO_3H-N(CH_3)_3$ complex at a series of fixed N-H distances, calculated at the MP2/6-311++G(df,pd) level of theory. At each point on the curve, all other structural parameters have been optimized.

coupling tensor of free TMA⁴⁴ onto the inertial axis system of the calculated structure gives a predicted value of χ_{aa} equal to -3.30 MHz, quite different from the observed value of -1.517

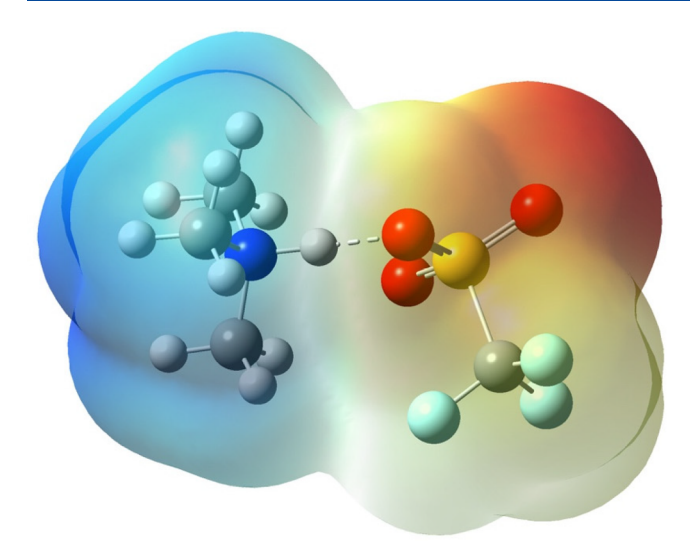


Figure 5. Optimized structure of trimethylammonium triflate obtained with MP2/6-311++G(df,pd) calculations, with an electrostatic potential map on the electron density surface. Regions in red indicate negative charge, and regions in blue indicate positive charge. The isovalue in the plot is 0.0004 au.

MHz. Likewise, for $(\chi_{bb} - \chi_{cc})$, the projected value is 0.65 MHz, which also differs significantly from the observed value of 0.092 MHz. These results suggest substantial electronic rearrangement of the TMA unit upon complexation but, taken alone, do not necessarily indicate that proton transfer is the cause. In this regard, we note that projecting the theoretical quadrupole coupling tensor for TMAH⁺ previously obtained at the B3LYP/6-311++G(3df,2p) level of theory⁴⁵ also gives poor agreement with the observed coupling constants of the complex, with projected values of χ_{aa} and $(\chi_{bb} - \chi_{cc})$ equal to -0.159 and 0.031 MHz, respectively. In this case, however,

polarization and charge transfer, which are not accounted for in an analysis based on projection, are expected to be especially important. Overall, it is apparent that a simple analysis based on projecting free, unperturbed monomer values of the ¹⁴N coupling constants is not a good way to proceed and needs to be replaced with comparisons based on full electronic structure calculations which automatically incorporate the full range of physical effects that can influence the electric field gradient at the ¹⁴N nucleus.

As noted above, Figure 6 shows that the observed values of χ_{aa} , χ_{bb} , and χ_{cc} are in excellent agreement with those calculated at an N-H distance of 1.093 Å. Moreover, it is clear that any significantly different choice of the distance would yield poorer agreement between the observed and calculated values. Because the sum of covalent radii⁴⁶ for nitrogen and hydrogen is 1.03 Å, this provides strong evidence that the observed coupling constants reflect complete or near-complete transfer of the triflic acid proton to the trimethylamine. Indeed, the N-H distance calculated at the MP2/6-311++G(df,pd) level for TMAH⁺ is 1.02 Å, indicating that the calculated value in the complex (1.09 Å) is quite close to that in the trimethylammonium cation. Complementing this viewpoint is the calculated O-H bond distance, which increases from 0.97 Å in free triflic acid to 1.459 Å in the complex (again with the MP2/6-311+ +G(df,pd) level/basis), the latter being much too long to imply the retention of a covalent O-H interaction in the adduct. Interestingly, while the location of the potential energy minimum at 1.093 Å is clear in Figure 4, the curve shows a slight inflection at long distances (~1.5 Å), which is perhaps reasonably regarded as a vestige of a minimum at the hydrogen-bonded geometry.

Inferences based on bond lengths can be further developed through use of the "proton transfer parameter", ρ_{PT} , which was first defined by Kurnig and Scheiner⁴⁷ for the study of amine—hydrogen halide complexes and later adapted in the study of

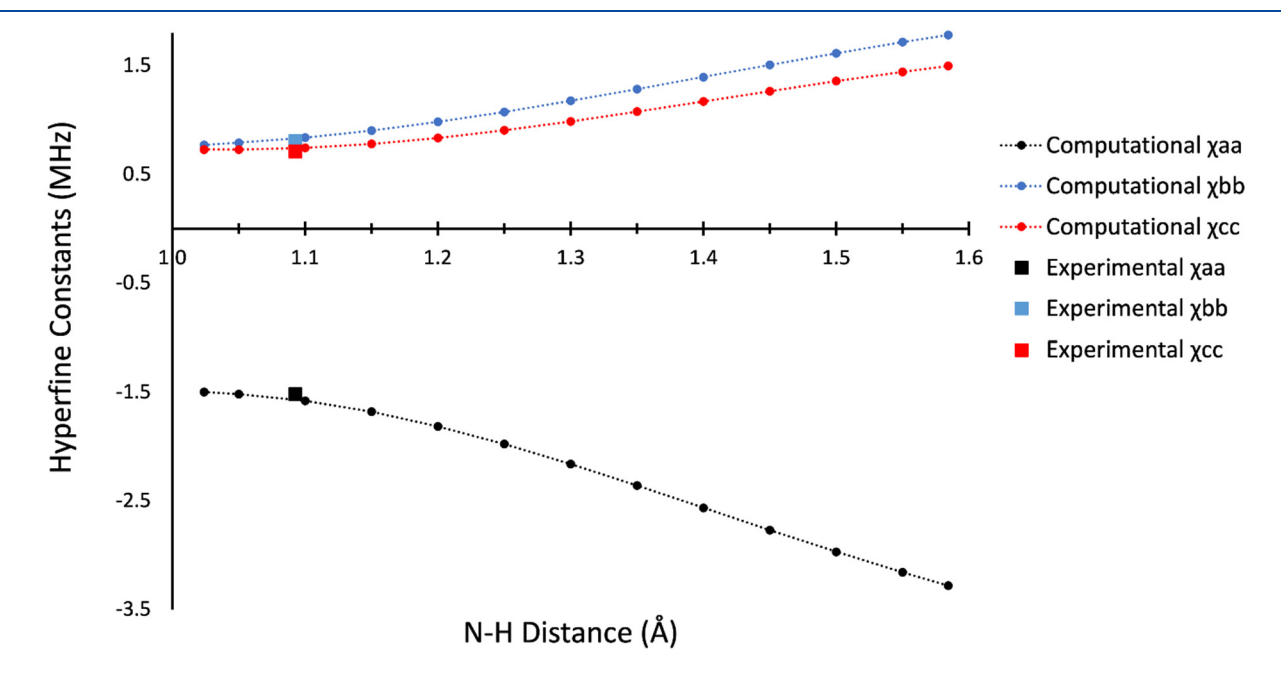


Figure 6. A plot showing the predicted ¹⁴N hyperfine constants at fixed N–H interatomic distances along the proton transfer coordinate with all remaining coordinates optimized. All values are from MP2/6-311++G(df,pd) calculations. The square points represent the experimentally determined hyperfine constants. These points are placed at an N–H interatomic distance of 1.093 Å, which is that obtained from the fully optimized structure at the same level of theory.

 $\mathrm{HNO_{3}}$ complexes. 20,22,23 For the triflic acid $-\mathrm{TMA}$ system, the definition takes the form

$$\rho_{\rm PT} = (r_{\rm OH}^{\rm complex} - r_{\rm OH}^{\rm free}) - (r_{\rm HN}^{\rm complex} - r_{\rm HN}^{\rm free}) \tag{1}$$

Here, $r_{\rm OH}^{\rm complex}$ and $r_{\rm HN}^{\rm complex}$ represent interatomic distances from the predicted complex structure, $r_{\rm OH}^{\rm free}$ represents the O–H interatomic distance for free triflic acid, and $r_{\rm HN}^{\rm free}$ represents the N–H interatomic distance in TMAH⁺. For a hydrogen-bonded complex, the first term is negligible and the second term is positive, giving $\rho_{\rm PT}$ a negative value. When proton transfer has taken place, the first term is positive and the second term is negligible, giving $\rho_{\rm PT}$ a positive value. Values of $\rho_{\rm PT}$ calculated are included in Table 2, where it may be seen that all levels of theory employed concur with the conclusion that proton transfer has taken place upon formation of the complex.

In addition, albeit less direct, evidence for proton transfer comes from the calculated dipole moment of the complex. At the MP2/6-311++G(df,pd) level of theory, the total dipole moment, $\mu_{\rm T}$, is 10.5 D (Table 2). This exceeds the sum of the calculated dipole moments of free TMA (0.9 D) and triflic acid (2.7 D) by 6.9 D, thus further indicating substantial charge separation upon complex formation. Such a separation is consistent with the visual representation of the charge distribution provided by the electrostatic potential map shown in Figure 5. There, it may be seen that the proton lies in the electropositive region of the complex which clearly resembles a TMAH⁺ cation.

Finally, simple energetic arguments make it possible to understand why triflic acid and trimethylamine would form an ion pair in the gas phase without the assistance of a microsolvent. These arguments are similar to those applied to amine—hydrogen halide¹⁷ and nitric acid—water complexes. From measured proton affinities, 48 we have

$$CF_3SO_3H \rightarrow H^+ + CF_3SO_3^- \quad \Delta H = 305 \text{ kcal/mol}$$
 (2)

$$TMA + H^{+} \rightarrow TMAH^{+}$$
 $\Delta H = -227 \text{ kcal/mol}$ (3)

Thus, the transfer of a proton from triflic acid to TMA to form TMAH⁺ and CF₃SO₃⁻ at infinite separation is endothermic by 78.2 kcal/mol. This endothermicity is offset, however, by the Coulomb energy associated with bringing the ions to their distance in the complex. There is, of course, some ambiguity in the choice of that distance, as the ions are not point charges. However, if we estimate it to be roughly the nitrogen-sulfur distance calculated from the Cartesian coordinates provided in the Supporting Information (3.356 Å), then the Coulomb energy $(q_1q_2/4\pi\epsilon_0 r)$, where q_1 and q_2 are unit charges of opposite sign and r is the distance) has a value of -99 kcal/mol. This brings the overall reaction energy to -21 kcal/mol, indicating an energetic favorability for transfer of the proton. Note that if, instead of using the nitrogen-sulfur distance, we distribute the negative charge of the CF₃SO₃⁻ moiety equally among the three oxygens (which bear the negative formal charge of the anion) and retain a unit positive charge on the nitrogen (since it bears the positive formal charge of the TMAH⁺ cation), the sum of the resulting Coulomb energies is −104 kcal/mol. This value is probably somewhat better than the -99 kcal/mol based on the N-S distance and brings the net interaction energy to -26 kcal/mol. Fortunately, the two methods of calculation are similar enough to provide some confidence that the result is not wildly dependent on the

chosen distance. A pictorial representation of the energetics is shown in Figure 7.

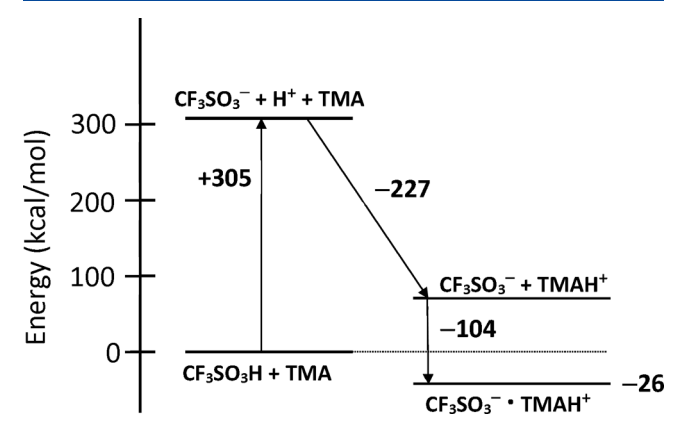


Figure 7. Energy diagram depicting the ionization of triflic acid (+305 kcal/mol), proton attachment to TMA (-227 kcal/mol), and the Coulomb energy, $q_1q_2/4\pi\epsilon_0r$ (-104 kcal/mol), combining to place the energy of the ion pair at 26 kcal/mol below that of the separated triflic acid and TMA. The first two steps are based on experimental proton affinity values. The third step is approximate, as described in the text. The energy of the final ion pair computed at the MP2/6-311++G(df,pd) level of theory is -31.4 kcal/mol. See the text for a discussion.

The energy change for complex formation of \sim -26 kcal/ mol estimated from this simple model is somewhat smaller in magnitude than the -31.4 kcal/mol computed at the MP2/6-311++G(df,pd) level of theory. A disparity is expected given the ambiguity associated with assigning a distance to ions that are not point charges and the neglect of effects such as polarization and distortion of the moieties. However, it suffices to provide an intuitive understanding of the energetics of ion pair formation in the gas phase. Note, however, that these arguments establish the stability of the ion pair relative to that of the isolated monomers but do not address the relative stabilities of the ion pair and the hydrogen-bonded form. Such a comparison is necessary to understand whether or not proton transfer should occur in the isolated complex. As seen in Figure 4, however, the hydrogen-bonded complex is a hypothetical species for this system, and thus its energy cannot be rigorously determined. Nevertheless, a binding energy of -26 kcal/mol (or -31.4 kcal/mol from full electronic structure calculations) is larger than that of a typical (non-proton-shared) hydrogen bond, 49 making the preference for ion pair formation entirely plausible.

Finally, it is interesting to note that the value of the deprotonation energy for triflic acid (305 kcal/mol) is significantly less than that of other common acids. For example, values for HNO₃ and HCl are 324 and 333 kcal/mol, respectively. These values would not predict a decisive preference for proton transfer by the above model. Specifically, in the case of HCl, the model predicts an ion pair energy of -12 kcal/mol relative to the isolated monomers, while for HNO₃, the predicted value is -3 kcal/mol relative to the isolated monomers. The former is quite comparable to an expected hydrogen bond energy while the latter is so close to zero that even its sign is not clear. Interestingly, HNO₃-TMA showed significant changes in the ¹⁴N quadrupole coupling constants which were interpreted as indicating partial, though not complete, proton transfer, and HCl-TMA has been

described as a proton-shared system.¹⁷ It seems logical to conclude that the strong acidity of triflic acid and its correspondingly low deprotonation energy underlie its ability to form a bare ion pair with TMA in the gas phase.

CONCLUSION

The microwave spectrum of the trimethylammonium triflate ion pair has been observed by chirped-pulse and cavity Fourier transform microwave spectroscopy using on-the-fly mixing of triflic acid and trimethylamine in a supersonic jet. A computational analysis of the complex indicates the formation of an ion pair resulting from complete or near-complete proton transfer from the acid to the base. A comparison of the computed hyperfine constants at different degrees of proton transfer with their experimentally determined values confirms this prediction. Simple energetic arguments based on proton affinities and Coulomb attraction readily rationalize the spontaneous ionization observed in the cold 1:1 complex.

ASSOCIATED CONTENT

Solution Supporting Information

The Supporting Information is available free of charge at https://pubs.acs.org/doi/10.1021/acs.jpca.1c03345.

Tables of observed transition frequencies, assignments, and residuals from the least-squares fits; Cartesian coordinates for the fully optimized structure at the MP2/6-311++G(df,pd) level of theory (PDF)

AUTHOR INFORMATION

Corresponding Author

Kenneth R. Leopold — Department of Chemistry, University of Minnesota, Minneapolis, Minnesota 55455, United States; orcid.org/0000-0003-0800-5458; Email: kleopold@umn.edu

Authors

Nathan Love — Department of Chemistry, University of Minnesota, Minneapolis, Minnesota 55455, United States Anna K. Huff — Department of Chemistry, University of Minnesota, Minneapolis, Minnesota 55455, United States

Complete contact information is available at: https://pubs.acs.org/10.1021/acs.jpca.1c03345

Notes

The authors declare no competing financial interest.

ACKNOWLEDGMENTS

This work was supported by the National Science Foundation (Grants CHE 1563324 and CHE 1953528) and the Minnesota Supercomputing Institute. N.L. was supported, in part, by a Lester C. and Joan Krogh-Excellence Fellowship at the University of Minnesota.

REFERENCES

- (1) Leopold, K. R. Hydrated Acid Clusters. *Annu. Rev. Phys. Chem.* 2011, 62, 327-349. and references therein.
- (2) Cheung, J. T.; Dixon, D. A.; Herschbach, D. R. Cluster Beam Chemistry: Adducts of Hydrogen Halides with Ammonia Clusters. *J. Phys. Chem.* **1988**, *92*, 2536–2541.
- (3) Breen, J. J.; Kilgore, S.; Wei, S.; Tzeng, W.-B.; Keesee, R. G.; Castleman, A. W., Jr. Reactions of Hydrogen Halides with Clusters of Ammonia Molecules. *J. Phys. Chem.* **1989**, *93*, 7703–7707.

- (4) Eustis, S. N.; Radisic, D.; Bowen, K. H.; Bachorz, R. A.; Haranczyk, M.; Schenter, G. K.; Gutowski, M. Electron-Driven Acid-Base Chemistry: Proton Transfer from Hydrogen Chloride to Ammonia. *Science* **2008**, *319*, 936–939.
- (5) Eustis, S. N.; Whiteside, A.; Wang, D.; Gutowski, M.; Bowen, K. H. Ammonia Hydrogen Bromide and Ammonia Hydrogen Iodide Complexes: Anion Photoelectron and Ab Initio Studies. *J. Phys. Chem.* A **2010**, *114*, 1357–1363.
- (6) Del Bene, J. E.; Jordan, M. J. T. What a Difference a Decade Makes: Progress in Ab Initio Studies of the Hydrogen Bond. *J. Mol. Struct.: THEOCHEM* **2001**, *573*, 11–23.
- (7) Jordan, M. J. T.; Del Bene, J. E. Unraveling Environmental Effects on Hydrogen-Bonded Complexes: Matrix Effects on the Structures and Proton-Stretching Frequencies of Hydrogen Halide Complexes with Ammonia and Trimethylamine. *J. Am. Chem. Soc.* **2000**, *122*, 2101–2115.
- (8) Brauer, C. S.; Craddock, M. B.; Kilian, J.; Grumstrup, E. M.; Orilall, M. C.; Mo, Y.; Gao, J.; Leopold, K. R. Amine Hydrogen Halide Complexes: Experimental Dipole Moments and a Theoretical Decomposition of Dipole Moments and Bond Energies. *J. Phys. Chem. A* **2006**, *110*, 10025–10034.
- (9) Barnes, A. J.; Latajka, Z.; Biczysko, M. Proton Transfer in Strongly Hydrogen-Bonded Molecular Complexes: Matrix Effects. *J. Mol. Struct.* **2002**, *614*, 11–21.
- (10) Scheiner, S. Hydrogen Bonding: A Theoretical Perspective; Oxford University Press: New York, 1997.
- (11) Theoretical Treatments of Hydrogen Bonding; Hadži, Ed.; John Wiley and Sons: Chichester, UK, 1997.
- (12) Proton Transfer in Hydrogen-Bonded Systems; Bountis, T., Ed.; NATO ASI Series, B: Physics Vol. 291; Plenum: New York, 1992.
- (13) Latajka, Z.; Scheiner, S.; Ratajczak, H. The Proton Position in Amine-HX (X = Br, I) Complexes. *Chem. Phys.* **1992**, 166, 85–96.
- (14) Mulliken, R. S.; Person, W. B. Molecular Complexes. A Lecture and Reprint Volume; Wiley-Interscience: New York, 1969.
- (15) Mulliken, R. S. Molecular Compounds and Their Spectra. III. The Interaction of Electron Donors and Acceptors. *J. Phys. Chem.* **1952**, *56*, 801.
- (16) Coulson, C. A. Valence; Oxford University Press: Glasgow, 1952.
- (17) Legon, A. C. The Nature of Ammonium and Methylammonium Halides in the Vapor Phase: Hydrogen Bonding versus Proton Transfer. *Chem. Soc. Rev.* **1993**, 22 (3), 153–163. and references therein.
- (18) Hunt, S. W.; Higgins, K. J.; Craddock, M. B.; Brauer, C. S.; Leopold, K. R. Influence of a Polar Near Neighbor on Incipient Proton Transfer in a Strongly Hydrogen Bonded Complex. *J. Am. Chem. Soc.* **2003**, *125*, 13850–13860.
- (19) Ott, M. E.; Leopold, K. R. A Microwave Study of the Ammonia Nitric Acid Complex. *J. Phys. Chem. A* **1999**, *103*, 1322–1328.
- (20) Sedo, G.; Leopold, K. R. Partial Proton Transfer in a Molecular Complex: Assessments from Both the Donor and Acceptor Points of View. *J. Phys. Chem. A* **2011**, *115*, 1787–1794.
- (21) Canagaratna, M.; Phillips, J. A.; Ott, M. E.; Leopold, K. R. The Nitric Acid Water Complex: Microwave Spectrum, Structure, and Tunneling. *J. Phys. Chem. A* **1998**, *102*, 1489–1497.
- (22) Craddock, M. B.; Brauer, C. S.; Leopold, K. R. Microwave Spectrum, Structure, and Internal Dynamics of the Nitric Acid Dihydrate Complex. *J. Phys. Chem. A* **2008**, *112*, 488–496.
- (23) Sedo, G.; Doran, J. L.; Leopold, K. R. Partial Proton Transfer in the Nitric Acid Trihydrate Complex. *J. Phys. Chem. A* **2009**, *113*, 11301–11310.
- (24) Kisiel, Z.; Pietrewicz, B. A.; Fowler, P. W.; Legon, A. C.; Steiner, E. Rotational Spectra of the Less Common Isotopomers, Electric Dipole Moment, and the Double Minimum Inversion Potential of H₂O···HCl. *J. Phys. Chem. A* **2000**, *104*, 6970–6978.
- (25) Kisiel, Z.; Białkowska-Jaworska, E.; Pszczółkowski, L.; Milet, A.; Struniewicz, C.; Moszynski, R.; Sadlej, J. Structure and Properties of the Weakly Bound Trimer (H₂O)₂HCl Observed by Rotational Spectroscopy. *J. Chem. Phys.* **2000**, *112*, 5767–5776.

- (26) Kisiel, Z.; Lesarri, A.; Neill, J. L.; Muckle, M. T.; Pate, B. H. Structure and Properties of the (HCl)₂H₂O Cluster Observed by Chirped-Pulse Fourier Transform Microwave Spectroscopy. *Phys. Chem. Chem. Phys.* **2011**, *13*, 13912–13919.
- (27) Legon, A. C.; Suckley, A. P. Bromine Nuclear Quadrupole and Hydrogen Bromine Nuclear Spin Nuclear Spin Coupling in the Rotational Spectrum of H₂O···HBr. *Chem. Phys. Lett.* **1988**, *150*, 153—158.
- (28) Kisiel, Z.; Pietrewicz, B. A.; Desyatnyk, O.; Pszczółkowski, L.; Struniewicz, I.; Sadlej, J. Structure and Properties of the Weakly Bound Cyclic Trimer (H₂O)₂HBr Observed by Rotational Spectroscopy. *J. Chem. Phys.* **2003**, *119*, 5907–5917.
- (29) McIntosh, A.; Walther, T.; Lucchese, R. R.; Bevan, J. W.; Suenram, R. D.; Legon, A. C. The Microwave Spectrum and Ground-State Structure of H.O.: HI. Chem. Phys. Lett. 1999, 314, 57–64.
- (30) Hammett, L. P.; Deyrup, A. J. A Series of Simple Basic Indicators. I. The Acidity Functions of Mixtures of Sulfuric and Perchloric Acids with Water. *J. Am. Chem. Soc.* **1932**, *54*, 2721–2739.
- (31) Himmel, D.; Goll, S. K.; Leito, I.; Krossing, I. A Unified PH Scale for All Phases. *Angew. Chem., Int. Ed.* **2010**, 49, 6885–6888.
- (32) Kazakova, A. N.; Vasilyev, A. V. Trifluoromethanesulfonic Acid in Organic Synthesis. Russ. J. Org. Chem. 2017, 53, 485–509.
- (33) Olah, G. A.; Prakash, G. K. S.; Sommer, J. Superacids. Science 1979, 206 (4414), 13-20.
- (34) Saito, S.; Saito, S.; Ohwada, T.; Shudo, K. The Hammett Acidity Function H_o of Trifluoromethanesulfonic Acid Trifluoroacetic Acid and Related Acid Systems. A Versatile Nonaqueous Acid System. *Chem. Pharm. Bull.* **1991**, *39*, 2718–2720.
- (35) Howells, R. D.; Mc Cown, J. D. Trifluoromethanesulfonic Acid and Derivatives. *Chem. Rev.* **1977**, *77*, 69–92.
- (36) Phillips, J. A.; Canagaratna, M.; Goodfriend, H.; Grushow, A.; Almlöf, J.; Leopold, K. R. Microwave and Ab Initio Investigation of HF-BF₃. *J. Am. Chem. Soc.* **1995**, *117*, 12549–12556.
- (37) Dewberry, C. T.; Mackenzie, R. B.; Green, S.; Leopold, K. R. 3D-Printed Slit Nozzles for Fourier Transform Microwave Spectroscopy. *Rev. Sci. Instrum.* **2015**, *86*, No. 065107.
- (38) Brown, G. G.; Dian, B. C.; Douglass, K. O.; Geyer, S. M.; Shipman, S. T.; Pate, B. H. A Broadband Fourier Transform Microwave Spectrometer Based on Chirped Pulse Excitation. *Rev. Sci. Instrum.* **2008**, *79*, No. 053103.
- (39) Balle, T. J.; Flygare, W. H. Fabry-Perot Cavity Pulsed Fourier Transform Microwave Spectrometer with a Pulsed Nozzle Particle Source. *Rev. Sci. Instrum.* 1981, 52, 33–45.
- (40) Canagaratna, M.; Phillips, J. A.; Goodfriend, H.; Leopold, K. R. Structure and Bonding of the Sulfamic Acid Zwitterion: Microwave Spectrum of ⁺H₃N·SO₃⁻. *J. Am. Chem. Soc.* **1996**, *118*, 5290–5295.
- (41) Huff, A. K.; Mackenzie, R. B.; Smith, C. J.; Leopold, K. R. Facile Formation of Acetic Sulfuric Anhydride: Microwave Spectrum, Internal Rotation, and Theoretical Calculations. *J. Phys. Chem. A* **2017**, *121*, 5659–5664.
- (42) Love, N.; Huff, A. K.; Leopold, K. R. A New Program for the Assignment and Fitting of Dense Rotational Spectra Based on Spectral Progressions: Application to the Microwave Spectrum of Pivalic Anhydride. *J. Mol. Spectrosc.* **2020**, *370*, 111294.
- (43) Frisch, M. J.; Trucks, G. W.; Schlegel, H. B.; Scuseria, G. E.; Robb, M. A.; Cheeseman, J. R.; Scalmani, G.; Barone, V.; Petersson, G. A.; Nakatsuji, X. L.; et al. *Gaussian 16*; Gaussian, Inc.: Wallingford, CT, 2016.
- (44) Rego, C. A.; Batten, R. C.; Legon, A. C. The Properties of the Hydrogen-Bonded Dimer (CH₃)₃N····HCN from an Investigation of its Rotational Spectrum. *J. Chem. Phys.* **1988**, *89*, *696*–702.
- (45) Domene, C. P.; Fowler, P. W.; Legon, A. C. ¹⁴N Electric Field Gradient in Trimethylamine Complexes as a Diagnostic for Formation of Ion Pairs. *Chem. Phys. Lett.* **1999**, 309, 463–470.
- (46) Pyykkö, P. Additive Covalent Radii for Single-, Double-, and Triple-Bonded Molecules and Tetrahedrally Bonded Crystals: A Summary. *J. Phys. Chem. A* **2015**, *119*, 2326–2337.

- (47) Kurnig, I. J.; Scheiner, S. Ab Initio Investigation of the Structure of Hydrogen Halide-Amine Complexes in the Gas Phase and in a Polarizable Medium. *Int. J. Quantum Chem.* 1987, 32, 47–56. (48) Lias, S. G., Bartmess, J. E., Liebman, J. F., Holmes, J. L., Levin, R. D., Mallard, W. G., Eds.; Ion Energetics Data. In *NIST Chemistry WebBook*; NIST Standard Reference Data Base, Number 69; National Institute of Standards and Technology: Gaithersburg, MD, http://webbook.nist.gov (retrieved March 19, 2021).
- (49) For example, in $HNO_3-(H_2O)_n$ complexes, each hydrogen bond has been estimated to contribute -10 kcal/mol to the overall binding energy of the complex.¹ In H_3N –HF, the calculated binding energy is -12.9 kcal/mol (-12.3 kcal/mol with counterpoise correction).¹⁸